Moroccan Journal of Chemistry
ISSN : 2351-812X

Mor. J. Chem., 2023, Volume 11, Issue 03, Page 623-644
https://revues.imist.ma/index.php/morjchem
https://doi.org/10.48317/IMIST.PRSM/ morjchem-v11i3.37787

Inhibition of corrosion of steel in 1 M HCl solution by polyphenol extract: Application for Steel used in the automotive industry in Morocco

Chami A. [1*], Benabbou R. [1], Taleb M. [2], Rais Z. [2], El Haji M. [1]

[1]*Laboratory of Advanced Research in Industrial Logistics and Engineering (LARILE), National High School of Electricity and Mechanics, Optimization of Industrial and Logistics Systems Team (OSIL), Department (GIL), University Hassan II, Casablanca, Morocco*

[2]*Engineering Laboratory of Electro-chemistry, Modelisation, and Environment (LIEME), Faculty of Science Dhar El Mahraz, Sidi Mohamed Ben Abdellah University, Fez, Morocco*

**Corresponding author, Email address: aziz.chami@ensem.ac.ma*

Received *05 Feb 2023,*
Revised *07 May 2023,*
Accepted *11 May 2023*

Citation*: Chami A., Benabbou R., Taleb M., Rais Z., El Haji M. (2023). Inhibition of corrosion of steel in 1 M HCl solution by polyphenol extract: Application for Steel used in the automotive industry in Morocco, Mor. J.Chem.,14(3), 623-644*

Abstract: An experimental study was carried out to measure the inhibitory efficiency of polyphenol extracted from vegetable water (MA) and polyphenol extracted from pomace (GO) as green corrosion inhibitors for high yield strength steel (AHLE) and mild steel (AD) in an acid solution hydrochloric 1 M. The experiments revealed that the MA and GO behaved as mixed type inhibitors. This study was performed using the weight loss method, potentiodynamic polarization (PDP) and electrochemical impedance spectroscopy (EIS). The MA inhibits corrosion of both AD and AHLE in 1M HCl. Inhibition efficiency increases with increasing inhibitor concentrations to reach a maximum value of 95.7% for steel AHLE and a maximum value of 95.50% for mild steel. For the GO it inhibits the corrosion of steel AHLE and mild steel in HCl 1M. The efficiency increases with increasing inhibitor concentrations to reach a maximum value of 96.68% for AD and a maximum value of 95.23% for AHLE. According to the Langmuir isothermal model, the inhibitors MA and GO were adsorbed on the steel surfaces AHLE and AD by physical and chemical bonds. SEM and EDX examinations have proven the formation of a protective layer of inhibitors adsorbed on the steel surface.

Keywords: Polyphenol; Ecological Inhibitors; Steel; Automotive; Corrosion

1. Introduction

Everything around us is susceptible to deterioration. When the irreversible deterioration of a metal takes place by chemical or electrochemical reaction with its environment, it is called corrosion. It is a constant and continuous problem, often difficult to completely eliminate. Corrosion affects most industrial sectors. It represents 5% of the manufacturing cost for the automotive sector (Akandi *et al.*, 2023). In fact, corrosion limits the lifespan of materials, causing numerous replacement costs and high productivity losses, which strongly penalizes several industrial sectors. As a result, predicting the behavior of metal structures in the face of corrosion represents an important scientific and technological challenge. The study of corrosion in the automotive sector is of paramount importance due to the direct and indirect losses caused by this scourge. Indeed, even if the car manufacturers have made great progress in protecting the hull and the paint from this damage via surface treatments and choice of

materials, the vehicles nevertheless remain exposed. Depending on the atmospheric conditions and the environmental environment, the materials are affected and lose the properties of their uses. The warranty period of a vehicle is an increasingly strong selling point. However, poor risk management can lead to considerable financial losses for a car manufacturer, so the duration of guarantees against bodywork perforation in Europe (Chami *et al.*, 2021), successively extended to 6, 8 and 12 years at the end of the 1990s , has led manufacturers to accelerate research into problems related to the appearance and development of corrosion. The bodywork protection methods are well known: galvanized sheets, generous application of glues and sealants, injection of wax into the hollow bodies (Li *et al.*, 2023). However, the sum of all these protections has two major drawbacks, which are the increase in manufacturing costs and the weight of the vehicles: the weight of the vehicles must indeed be controlled to comply with European anti-pollution standards. To avoid these disadvantages and achieve 12 years of protection against corrosion, it is necessary to rationalize the technical choices, and therefore to work on the protection of steels by the use of environmentally friendly and inexpensive solutions. Indeed, the requirements of respect for the environment by the reduction of CO_2 emissions on the one hand and the continuous desire to reduce costs pushes manufacturers to seek inventive solutions (Leach *et al.*, 2020). The green inhibitors used to fight corrosion are the ideal candidates to meet this need, apart from the fact that they are inexpensive and respectful of the environment. In terms of protection against corrosion, it is possible to act on the material itself (judicious choice, suitable shapes, constraints depending on the applications, etc.), on the surface of the material (coating, paint, any type of surface treatment, etc.) or on the environment with which the material is in contact (corrosion inhibitors). The use of inhibitors to prevent the dissolution process of metals remains an inevitable and widespread application. In fact, inhibitors are chemical substances which, when added in small quantities to the environment, reduce the rate of corrosion of materials. Beyond its protective power, the choice of an inhibitor must take into consideration the health and safety constraints, the impact on the environment, as well as order criteria. economic (availability and cost) (Mbamalu *et al.*, 2023; Elmsellem *et al.*, 2014; Zerfaoui *et al.*, 2014). Most of the inhibitors known today are organic compounds that adsorb onto the steel surface and decrease the rate of corrosion by blocking the active sites, but the majority of these compounds are expensive, toxic, and pose a fundamental problem for the environment. Thus, the use of natural products as barriers against the spread of harmful synthetic chemicals has become an ecological necessity that is gaining great interest in the world. This type of inhibitors does not contain heavy metals or toxic compounds, they are biodegradable and renewable. Several studies show that the use of these products (oils and plant extracts) as a source of green inhibitors for the protection of metals makes it possible to achieve a very high rate of effectiveness (Al-Mazaideh *et al.*, 2018; Torres *et al.*, 2023; Chaubey *et al.*, 2014). It is in this context that this work complements previous work and focuses on the inhibition of the corrosion of steel used in automobile bodywork in an acid medium of 1M HCl by molecules derived from plants in a process of compliance with environmental standards (Chami *et al.*, 2020; 2021; 2022).

This study was carried out with the aim of studying the inhibition efficiency of the polyphenol extracted from vegetable waters and olive pomace using electrochemical techniques, and confirmed by a surface analysis characterization approach.

2. Experimental

2.1 Materials and methods

In our previous research work we carried out a statistical study and a survey of 100 professionals in the Moroccan automotive industry to identify the steel most affected by corrosion in the car and the

area of the bodywork most damaged. The results of this investigation show that the corrosion of automotive bodies depends on several variables: the area of the vehicle, the type of vehicle, the cause of corrosion, the type of corrosion and the region. The combination of these variables shows that localized pitting corrosion in the engine compartment accounts for the majority of vehicle corrosion cases. The statistical study shows that the high yield strength steel (AHLE) and mild steel (AD) are the most affected by corrosion in the car body.

Therefor the steel samples that are used for this study are (AHLE) and (AD). The steel samples intended for the tests were taken from the engine compartment of a vehicle over 5 years old; this choice follows the results of a survey of 100 professionals in the automotive industry in Morocco (Chami *et al*., 2021).

The electrolyte used is a molar solution of hydrochloric acid (1M HCl) is obtained by diluting the concentrated acid 37% by weight in distilled water. The steel specimens used in the experiments measured 15 mm × 10 mm. In addition, (AD) has the following chemical composition by weight: (0.09% P, 0.38% Si, 0.01% Al, 0.05% Mn, 0.21% C, 0.05% S and the balance iron). And (AHLE) has the chemical following composition: (0.03% P, 0.04% Si, 0.02% Al, 0.40% Mn, 0.08% C, 0.03% S, 0.15 (Nb+Ti) and the balance iron).

In order to obtain reliable results, the samples (AD) and (AHLE) are prepared before the test by polishing with grit sandpaper (grade 100-400-800-600-1200), followed by rinsing with distilled water, then dried under a stream of air.

2.2 Polyphenol usage protocol

This study concerns two types of inhibitors: the polyphenol extracted from olive water and the polyphenol extracted from pomace. The extraction of the polyphenol was carried out at the Laboratory of Engineers in Electrochemistry, Modeling and Environment, Faculty of Sciences Dhar El Mahraz, University Sidi Mohamed Ben Abdellah, Fez, Morocco (LIEME). The method used for the extraction of polyphenols is the same as that used by E. Marco (2007) with some modifications. It consists of putting 10 ml of sample in a centrifuge tube and then adding 15 ml of hexane. The solution obtained is stirred and then centrifuged for 5 min at 3000 (4000) rpm. The solution obtained consists of two phases which have been separated by elimination of the lipid part (upper phase). The same operations are repeated twice. Then a sample of 10 ml of the solution obtained is taken and then washed. Then 10 ml of ethyl acetate are added to the solution. The solution obtained is then stirred and centrifuged for 5 to 10 min at 3000 (4000) rpm. At the end the two phases are separated by recovering the upper phase. The operations are repeated 3 times. The ethyl acetate is evaporated and finally the residue is diluted in 3 ml of methanol.

2.3 Measurement method

In this study we used standard methods to measure the effectiveness of inhibitors. First the gravimetric method which is the first approach to the study of corrosion inhibition. It has the advantage of being easy to implement and requires only simple equipment. This method is based on the measurement of the loss of mass undergone by the steel samples which have been immersed in a solution of hydrochloric acid HCl 1 M at a given temperature. The second method is the stationary method (electrochemical polarization), it allows to obtain information on the slowest stage of the electrochemical process characteristic of the metal-solution interface in a relatively fast time compared to non-electrochemical methods. The third method is the transient electrochemical method based on the determination of the electrochemical impedance. It makes it possible to approach the various processes which can intervene during the inhibition of the corrosion of steel in acid medium.

2.3.1. *Gravimetric study*

The gravimetric test was carried out by immersing the mild steel sample and the HLE steel in a solution of 100 ml 1 M HCl without and with variable concentrations of the two inhibitors at 25°C in the thermostat. The dimensions of the steel samples are (1.5 cm x 1.5 cm) They are immersed vertically for 6 h in the 1 M Hcl solution at 25 °C. After 6 h of immersion the samples are washed with water and acetone, dried and weighed again. The corrosion rate (CR) is given by the relationship **Eqn. 1**:

$$CR = W/At \qquad \textbf{Eqn. 1}$$

With W is the weight loss in (mg) and A is the surface of the sample in (Cm^2) and t the immersion time (h-1). The inhibition efficiency of a compound is determined by the formula **Eqn. 2**:

$$EW(\%) = \left(\frac{CR - CR_{inh}}{CR}\right) \times 100\% \qquad \textbf{Eqn. 2}$$

Where CR and CR_{inh} denote the obtained corrosion rates in the nonexistence and existence of inhibitors.

2.3.2. *Electrochemical measurements*

Electrochemical experiments were recorded using a potentiostat (Biologic SP 200), coupled to a computer equipped with EC-Lab software. The working electrode is made of steel with an adjacent area value of 1.5 cm2. Before each experiment, the electrode is polished using emery paper to grade 1200. After that, the electrode is cleaned with distilled water. An Ag/AgCl electrode is used as a reference. All potentials are given with reference to this electrode. The counter electrode is a platinum plate. The aggressive medium used here is a 1M HCl solution prepared with concentrated HCl and distilled water (Salhi *et al.*, 2016; Ugi *et al.*, 2021; Rbaa *et al.*, 2019; El Faydy *et al.*, 2019; Laabaissi *et al.*, 2019; Ouakki *et al.*, 2019).

2.3.2.1. *Polarisation measurements.*

All potentials are with reference to the Ag/AgCl electrode. The counter electrode is platinum. The working electrode is immersed in the test solution for 30 min until a steady state open circuit potential was obtained. The polarization curve is recorded by polarization from −800 mV to -200 mV under potentiodynamic conditions corresponding to 1 mV/s (scanning speed) and under an air atmosphere. E% is calculated using equation **Eqn. 3**:

$$EI(\%) = \left(\frac{I_{corr} - I_{corr\ inh}}{I_{corr}}\right) \times 100\% \qquad \textbf{Eqn. 3}$$

where I_{corr} and $I_{corr\ inh}$ are the corrosion current density values without and with inhibitor, respectively.

2.3.2.2. *Impedance spectroscopy measurements.*

The electrochemical impedance spectroscopy measurements were carried out using a transfer function analyser (Biologic SP 200), with a small amplitude ac. Signal (10 mV), over a frequency domain from 100 KHz to 10 mHz at 25 °C and an air atmosphere. The transfer resistance R_{ct}, is obtained from the diameter of the semicircle in Nyquist representation. In this case, the inhibition efficiency is calculated using charge transfer resistance from Equation **Eqn. 4**:

$$ER\% = \frac{R_{ct} - R_{ct\ inh}}{R_{ct}} \times 100\% \qquad \textbf{Eqn. 4}$$

where $R_{ct(inh)}$ and R_{ct} are the charge transfer resistance in the presence and absence of inhibitor respectively (Saraswat *et al.*, 2022; Tan *et al.*, 2022; Bouayad *et al.*, 2017; Ghazoui *et al.*, 2017).

3. Results and Discussion

3.1 The effect of inhibitors MA and GO on HLE steel

3.1.1 Polarization method: inhibitor MA

Table 1 groups together the electrochemical parameters deduced from the polarization curves: the corrosion potential (E_{corr}), the corrosion current density (I_{corr}), the cathodic slope of Tafel (β_c) and the inhibition efficiency E (%) for different concentrations of the inhibitor.

Table 1. Electrochemical parameters derived from polarization curves for steel HLE in 1.0 M HCl solution with and without the addition of different concentrations of MA inhibitor.

Medium	Concentration (M)	$-E_{corr}$ (mV/ECS)	I_{corr} ($\mu A.cm^{-2}$)	$-\beta_c$ ($mV.dec^{-1}$)	IE%
1M HCl	---	406	791	151	
M / HLE	1	416	34	128	95.70
	0.75	406	57	135	92.27
	0.5	402	78	143	90.13
	0.25	383	264	133	66.62

As the concentration of the inhibitor increases, the corrosion density value (Icorr) decreases and the inhibition efficiency increases and reaches a maximum value of 95.70 % at 1g/l for the inhibitor MA. This can be justified by the increase in the rate of coverage of the surface by the adsorption of the inhibitor studied. In the presence of the inhibitor, the anodic and cathodic region exhibit a wide range of linearity, indicating that Tafel's law is well verified in both domains (**Figure 1**). Analysis of the cathodic slope values reveals a slight modification induced by the addition of the inhibitor. This suggests that the inhibitor studied acts on the cathodic reaction by simply blocking the available surface without affecting the reduction mechanism.

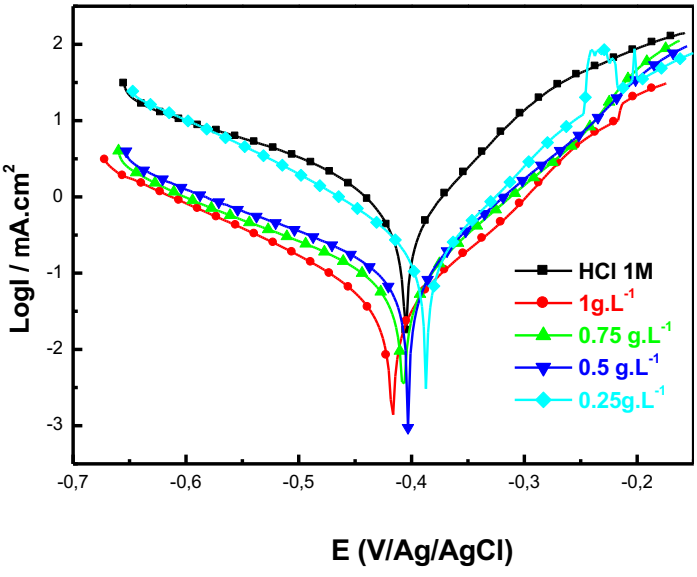

Figure 1. Polarization curves of steel in 1 M HCl solution containing different concentrations of MA inhibitor at 25°C

3.1.1.2 Impedance method: inhibitor MA

The impedance measurements were carried out using electrochemical impedance spectroscopy (EIS) at the corrosion potential, the frequency range chosen is from 100 KHz to 100 mHz with a sinusoidal excitation of 10 mV amplitude. The Nyquist representation consists in carrying on an

orthonormal reference the imaginary part $-Z_{im}$ according to the real part of the impedance Z_{Re} for the different frequencies. HLE steel is studied in a 1 M HCl solution in the absence and presence of the inhibitor MA by EIS after emersion for 30 min at 25C°. The **Figure 2** shows the Nyquist plot. The open circuit potential equivalent is shown in **Figure 3**. It should be noted that the plot is in the form of a semi-circle centered on the real axis which shows that the corrosion of HLE steel is caused by the load transfer of the corrosion mechanism (Bourichi *et al.*, 2016; EL Aoufir *et al.*, 2016; El Ouali *et al.*, 2013; Belghiti *et al.*, 2017; El aoufir *et al.*, 2017).

In the **Figure 2**, it can be seen that the Nyquist diagram shows an increase in the size of the semicircles with the increase in the concentration of the inhibitor MA. This increase shows that an absorption of the inhibitor MA on the surface of HLE steel. The equivalent circuit shown in the **Figure 3** can be modeled. In this equivalent circuit, a constant phase element CPE is used to replace a capacitive element to acquire a more accurate fit of experimental data. The CPE impedance is defined by two values, Q and n:

$$CPE = Q(iw)^n$$

Where Q and n ($0 < n < 1$) are frequency independent.

The equivalent circuit (**Figure 3)** allowed us to determine the parameters associated with the Nyquist plots (R_s, R_{ct}, C_{dl}, n_{dl}, Q, IE_{EIS}) the results are presented in **Table 2**.

Table 2. Electrochemical parameters derived from impedance curves for HLE steel in 1.0 M HCl solution with and without the addition of different concentrations of MA inhibitor at 25°C.

Medium	C (g/l)	R_s ($\Omega.cm^2$)	R_{ct} ($\Omega.cm^2$)	C_{dl} ($\mu F\ cm^{-2}$)	n_{dl}	Q ($\mu F.sn^{-1}$)	IE_{EIS} (%)
HCl 1M	-	0.739	37.29	103.9	0.777	249.2	---
M/AHLE	1	3.516	493.6	39.8	0.870	74.32	92.44
	0.75	0.727	328.4	42.26	0.842	109.6	88.64
	0.5	0.902	248.4	43.85	0.841	113.9	74.22
	0.25	1.044	86.64	81.04	0.788	154.1	56.95

It is clear from the results of **Table 2** that the increase in the concentration of the inhibitor MA is followed by the increase in the value of the resistance (R_{ct}), while the values of C_{dl} decrease. The increase in R_{ct} is related to the absorption of the inhibitor on the surface of the HLE steel, and therefore 7related to the formation of a protective layer (Chetouani *et al.*, 2002; Verma *et al.*, 1917; Guo *et al.*, 2013; Laabaissi *et al.*, 2019; Chai *et al.*, 2019). Moreover, the values of n increase with the concentration of inhibitor, which could be related to the decrease in surface heterogeneity resulting from the formation of an effective barrier against the aggressive medium and adsorption on the sites of most active adsorption. The order of inhibition efficiency from EIS measurements is in good agreement with those obtained from polarization.

3.1.1.3 Representation of impedance diagrams in the Bode plane

In order to acquire more information on the corrosion mechanisms and improve the previous results, the bode plots of the HLE steel in 1.0 M HCl without and with different concentrations of MA inhibitor at 25°C are shown in The **Figure 4**. It is clear from the **Figure. 4** the Bode representation shows the logarithm of the impedance modulus log|Z| and the phase angle as a function of frequency in a log f logarithmic scale. The phase angle plots become significantly broader in the high frequency range with increasing MA concentration. In any case, it is clear that the Bode phase angle plots have

only a single maximum, i.e. a time constant corresponds to a corrosion process by adsorption on the steel/solution interface

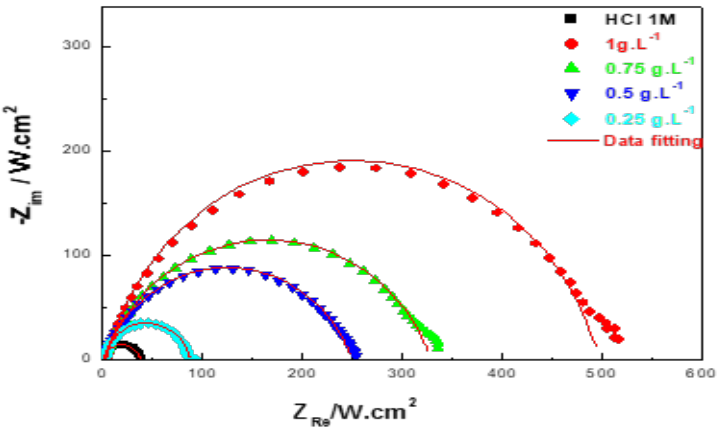

Figure 2. Nyquist curves of HLE steel in 1 M HCl solution containing different concentrations of MA inhibitor at 25°C.

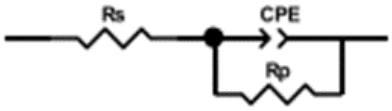

Figure 3. Equivalent electrical circuit proposed to model the steel interface HLE / HCl 1M + 1g/l of MA.

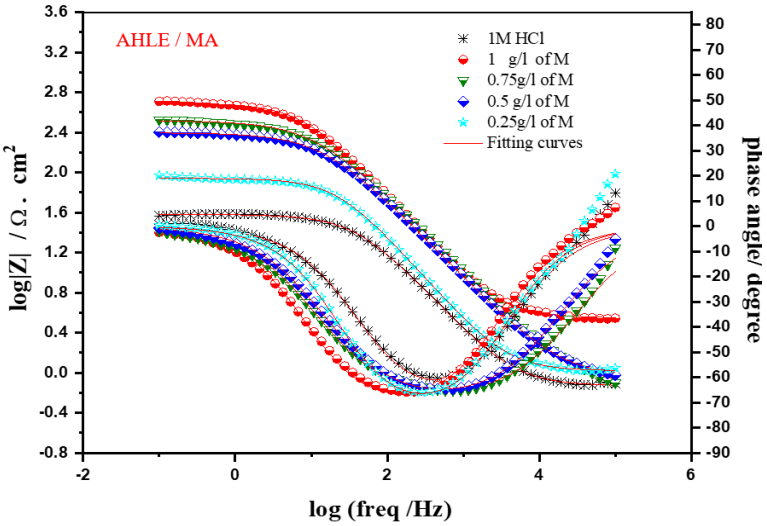

Figure 4. Bode representation of HLE steel in a 1 M HCl solution containing different concentrations of M inhibitor at 25°C

3.1.2 The effect of the inhibitors GO on HLE steel

A second study of the effect of the GO inhibitor on HLE steel in the same corrosive environment was carried out. The same previous techniques and methods were used. The results are presented in **Figures 5 &6 and Tables 3 & 4**

3.1.2.1 Polarization method: inhibitor GO

The electrochemical parameters deduced from the polarization curves are presented in the **Table 3**: the corrosion potential (Ecorr), the corrosion current density (Icorr), the cathodic slope of Tafel (βc) and

the inhibition efficiency E (%) for different concentrations of the inhibitor.c) and the inhibition efficiency E (%) for different concentrations of the inhibitor. The polarization curves of steel in 1 M HCl solution containing different concentrations of GO inhibitor at 25°C is shown in **Figure 4**.

Table 3. Electrochemical parameters from polarization curves for HLE steel in 1.0 M HCl solution with and without the addition of different concentrations of GO inhibitor

Medium	Concentration(M)	$-E_{corr}$ (mV/ECS)	I_{corr} ($\mu A.cm^{-2}$)	$-\beta_c$ ($mV.dec^{-1}$)	IE%
1M HCl	---	406	791	151	
GO /HLE	1	416	37	127	**95.23**
	0.75	400	55	153	**93.04**
	0.5	401	58	149	**92.66**
	0.25	395	178	129	**77.49**

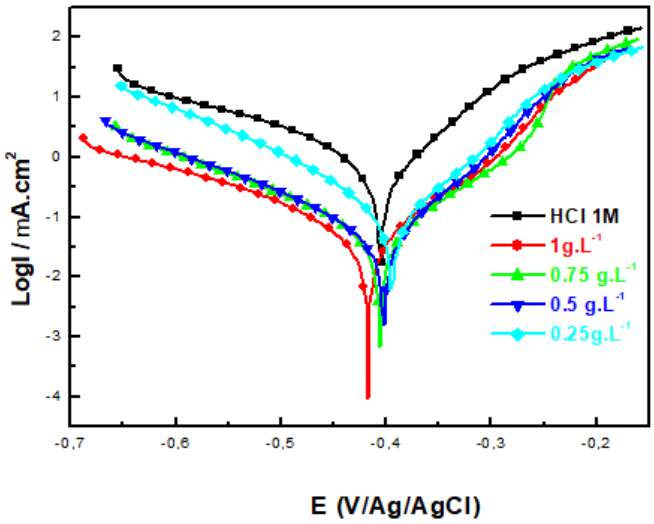

Figure 5. Polarization curves of HLE steel in 1 M HCl solution containing different concentrations of GO inhibitor at 25°C.

3.1.2.2 Impedance method: inhibitor GO

The electrochemical parameters derived from impedance curves for HLE steel in 1M HCl solution with and without the addition of different concentrations of GO inhibitor at 25°C.is shown in the **Table 4.**

Table 4. Electrochemical parameters from impedance curves for steel HLE in a 1.0 M HCl solution with and without the addition of different concentrations of I GO inhibitor at 25°C

Medium	C (g/l)	R_s ($\Omega.cm^2$)	R_{ct} ($\Omega.cm^2$)	C_{dl} ($\mu F\ cm^{-2}$)	n_{dl}	Q ($\mu F.sn-1$)	IEEIS (%)
HCl 1M	-	0.739	37.29	103.9	0.842	249.2	---
M/AHLE	1	3.516	493.6	39.8	0.841	74.32	**92.44**
	0.75	0.727	328.4	42.26	0.777	109.6	**88.64**
	0.5	0.902	248.4	43.85	0.788	113.9	**74.22**
	0.25	1.044	86.64	81.04	0.870	154.1	**56.95**

It is clear from the results of the **Table 4** that the increase in the concentration of the inhibitor GO is followed by the increase in the value of the resistance (R_{ct}). In the **Figure 5**, it can be seen that the Nyquist diagram shows an increase in the size of the semicircles with the increase in the concentration of the inhibitor GO. This increase shows that an absorption of the inhibitor GO on the surface of HLE steel.

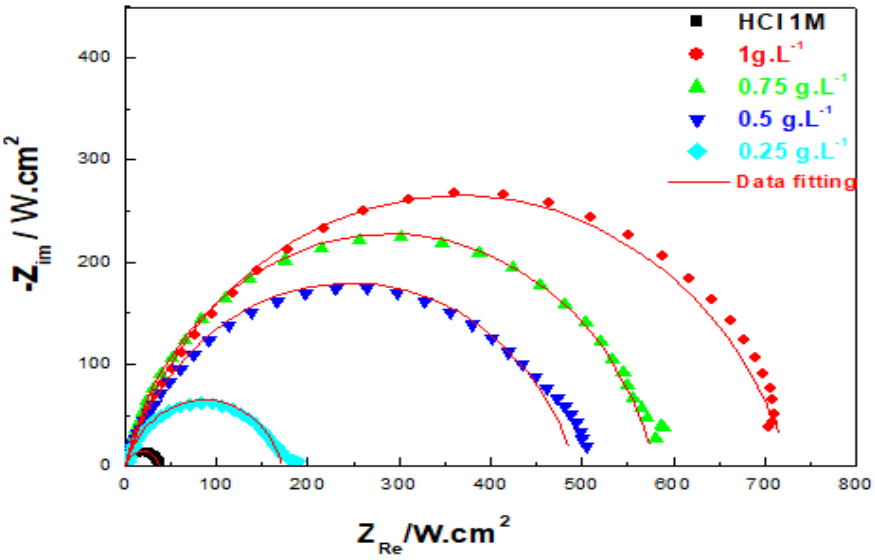

Figure 6. Nyquist curves of HLE steel in 1 M HCl solution containing different concentrations of GO inhibitor at 25°C.

On the basis of the study results of the effectiveness of the GO inhibitor on HLE steel in the corrosive medium HCl 1M **Figures (4 & 5)** and **Tables (3&4)**, it is noted that the inhibitor GO has a maximum efficiency of 95.23 and its behavior is similar to that of the inhibitor MA.

3.1.2.3 Representation of impedance diagrams in the Bode plane

In order to acquire more information on the corrosion mechanisms and improve the previous results, the bode plots of the HLE steel in 1.0 M HCl without and with different concentrations of GO inhibitor at 25°C are shown in the **Figure 7**. It is clear from the **Figure 7** that the phase angle plots become significantly broader in the high frequency range with increasing GO inhibitor concentration. In any case, it is clear that the Bode phase angle plots have only a single maximum, i.e. a time constant corresponds to a corrosion process by adsorption on the steel/solution interface.

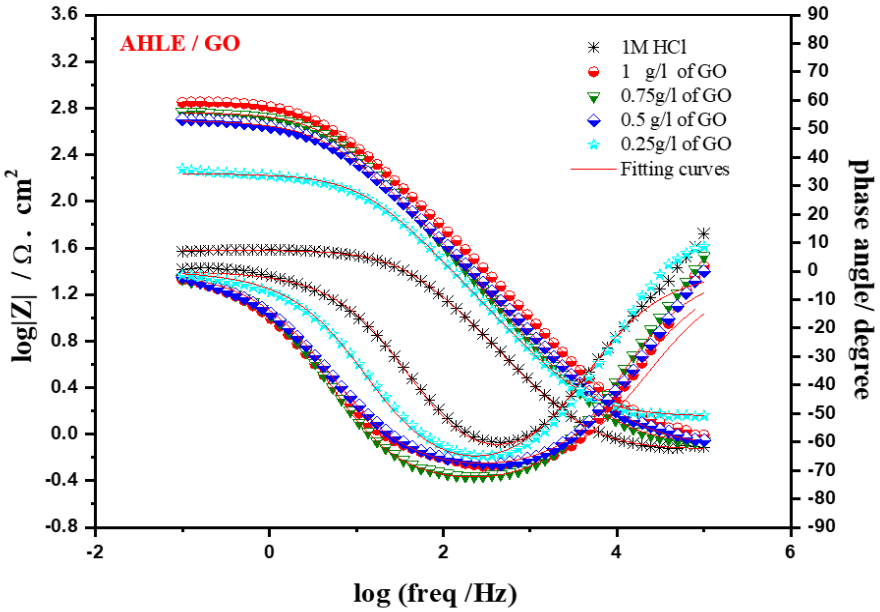

Figure 7. Bode representation of HLE steel in a 1 M HCl solution containing different concentrations of GO inhibitor at 25°C

3.2 The effect of the inhibitors MA and GO on mild steel

3.2.1 The effect of MA inhibitor on mild steel

3.2.1.1 Impedance method

In order to better understand the phenomenon occurring at the metal-solution interface in the presence of different concentrations of inhibitor, and in order to have more information on the phenomenon of corrosion inhibition of mild steel in the solution 1M HCl acid, we carried out impedance measurements in the Nyquist planes (**Figure 8**), in the absence and in the presence of MA compound at different concentrations under the same experimental conditions. These measurements make it possible to shed light on certain reaction mechanisms in the elementary processes (charge transfer, diffusion, adsorption) and from the impedance diagrams, we have access to the charge transfer resistance (R_{ct}) and to the capacitance of the double layer (C_{dl}) and therefore to the inhibition rate (inhibitory efficacy) under the operating conditions used (**Table 5**). R_{ct} is calculated from the impedance difference at high and low frequencies on the real axis, as suggested by Tsuru and Haruyama (Musa *et al.*, 2012; Dermeche *et al.*, 2013; El Faydy *et al.*, 2021). In our case, the electrochemical impedance spectroscopy (EIS) measurements were carried out in potentiostatic mode at the corrosion potential at 25 C° after 30 min of immersion. The capacitance of the double layer C_{dl} is determined at the frequency at which the imaginary part of the impedance is maximum. Measurements by electrochemical impedance spectroscopy carried out at the steel/1M HCl interface without and with addition of MA inhibitor at different concentrations result in the Nyquist diagrams shown in the **Figure 6.** These plots show that the curves have a well-defined capacitive loop that only increases in size (diameter) with increasing inhibitor concentration, indicating an increase in inhibitory capacity. The presence of a single capacitive loop indicates that mild steel corrosion is primarily controlled by an electronic charge transfer process. The results show the formation of a single capacitive loop for all impedance patterns by forming a protective layer on the metal surface, leading to the corrosion inhibition process. In practice, the impedance diagrams obtained are not centered on the real axis (the semi-circles are imperfect), and this is attributed to the difference in frequency dispersion (About *et al.*, 2021; Popoola *et al.*, 2014). To which heterogeneity can be linked. of the metal surface that generates a reaction rate distribution. The decrease in C_{dl} value with the addition of our inhibitor indicates the formation of a protective layer due to the adsorption of the inhibitor to the metal surface as a result of the displacement of molecules from the surface by MA.

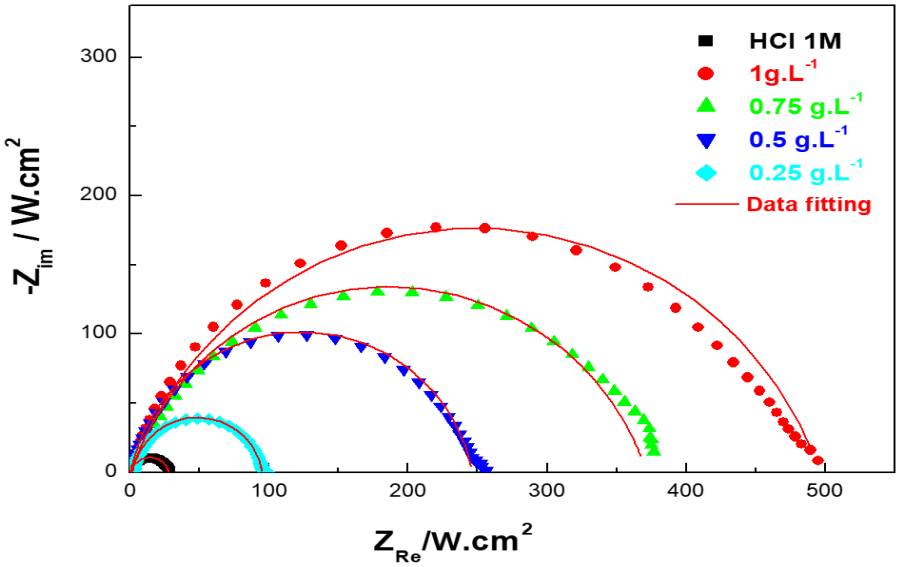

Figure 8. Nyquist curves of mild steel in a 1 M HCl solution at different concentrations of MA inhibitor at 25°C

The electrochemical impedance spectroscopy study is in good agreement with the result obtained by the weight loss measurements and polarization curves. the effectiveness of the studied MA shows that with the increase in concentration, there will be a decrease in the C_{dl} value and an increase in the values of R_{ct} and E (%). The efficiency reaches its maximum value of 94.30%.

Table 5. Electrochemical parameters from impedance curves for mild steel in 1 M HCl solution with and without the addition of different concentrations of MA inhibitor at 25°C

Medium	C (g/l)	R_s ($\Omega.cm^2$)	R_{ct} ($\Omega.cm^2$)	C_{dl} ($\mu F\ cm^{-2}$)	n_{dl}	Q ($\mu F.sn^{-1}$)	IE_{EIS} (%)
1M HCl	-	0.808	27.55	105.4	0.843	263.2	**---**
M/ AD	1	1.079	495.4	53.25	0.788	114.7	**94.43**
	0.75	1.036	370.7	64.65	0.799	136.8	**92.56**
	0.5	0.889	245.5	71.95	0.880	116.5	**88.77**
	0.25	2.15	93.43	77.61	0.895	129.8	**70.51**

3.2.1.2 Representation of impedance diagrams in the Bode plane

In order to acquire more information on the corrosion mechanisms and improve the previous results, bode plots of mild steel in 1 M HCl without and with different concentrations of MA inhibitor at 25°C are shown in the (**Figure 7**).

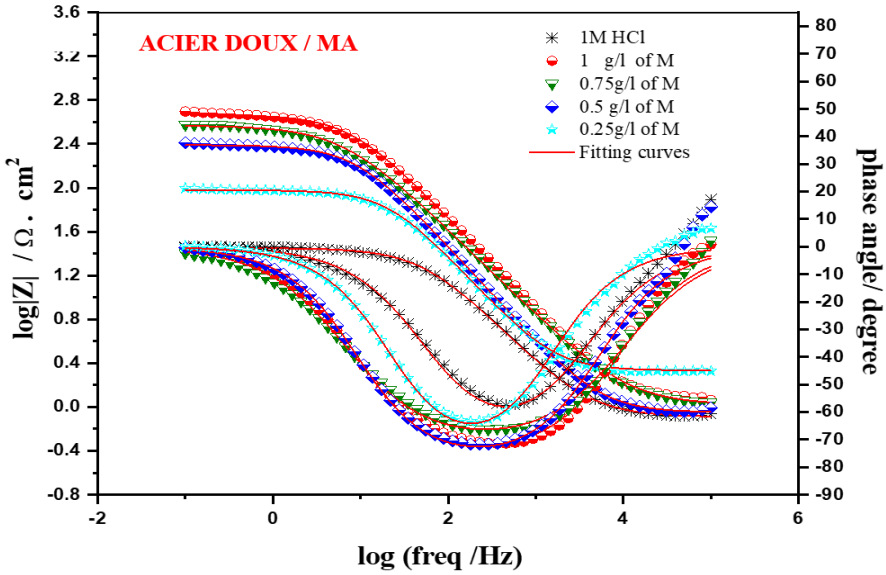

Figure 9. bode representation of mild steel in a 1 M HCl solution containing different concentrations of MA inhibitor at 25°C.

It can be seen from the **Figure 9** that the phase angle plots become significantly broader in the high frequency range with increasing MA inhibitor concentration. In any case, it is clear that the Bode phase angle diagrams have only one maximum, i.e. a time constant corresponds to an adsorption corrosion process on the steel/solution interface.

3.2.1.3 Polarization method

The effect of the MA inhibitor on the anodic or cathodic reactions was analyzed more precisely by performing a potentiodynamic polarization test. **Figure 8** shows the polarization curves after 30 min of immersion in the solutions containing the inhibitor and blank. Using the Tafel extrapolation method, polarization parameters including E_{corr}, i_{corr}, $ß_a$ and $ß_c$ are measured and reported in **Table 6**. Corrosion inhibition effectiveness was derived as shown below:

$$E_i\ \% = \frac{I_{corr,0} - I_{corr,0_{MA}}}{I_{corr,0}} \times 100\% \qquad \textbf{Eqn. 5}$$

where $I_{corr,\ 0}$, and $I_{corr,\ MA}$ represent the corrosion current densities without counting and by means of the existence of MA can be observed from the **Figure 8** and **Table 6** that anodic and cathodic corrosion current densities decrease in the presence of MA inhibitor, suggesting inhibition of anodic electrodissolution and cathodic progression of hydrogen. This shows a reduction in the rate of electrochemical reactions, which can be attributed to the adsorption of MA inhibitor molecules and the formation of a protective film on the metal surface (Abdulbasit *et al.*, 2023), (Abubakar *et al.*, 2019), (Ezeh, *et al.*, 2023). It can also be observed that cathodic processes are suppressed to a greater extent compared to anodic processes, indicating a cathodic predominance of MA inhibitor.

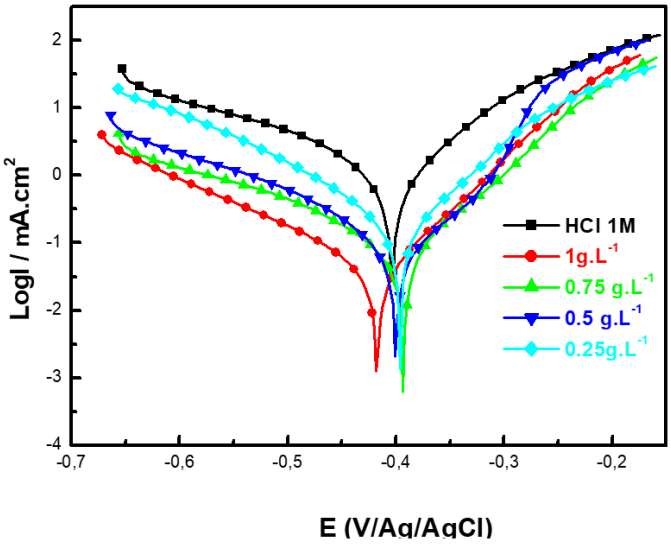

Figure 10. Polarization curves of mild steel in a 1 M HCl at different concentrations of MA inhibitor

Moreover, the cathode branches of Tafel represent parallel lines (**Figure 10**), suggesting that MA inhibitor does not alter the mechanism of hydrogen evolution and suggests that the reduction of hydrogen ions proceeds mainly via a transfer mechanism charging (Abdulbasit *et al.*, 2023). The inhibitory efficacy (Ei (%)) increases with the MA inhibitor concentration reaching its maximum 95.50% at 10^{-3} M (**Table 6**). The polarization data are in agreement with the gravimetric ones; This allows us to have more information on the inhibitory action of the molecule tested.

Table 6. Electrochemical parameters derived from polarization curves for mild steel in 1.0 M HCl solution **with** and without the addition of different concentrations of MA inhibitor.

Medium	Concentration(M)	-E_{corr} (mV/ECS)	I_{corr} (µA.cm−2)	-β_c (mV.dec−1)	IE%
1M HCl	---	403	978	138	
M /AD	1	414	44	140	**95.50**
	0.75	390	72	136	**92.63**
	0.5	399	116	139	**88.13**
	0.25	397	263	132	**73.10**

3.2.2 The effect of GO inhibitor on mild steel

3.2.2.1 Impedance method

The corrosion behavior of mild steel in the presence of GO has also been studied by EIS. A typical set of Nyquist diagrams is shown in **Figure 8.** The values of the associated electrochemical

parameters and the corrosion inhibition efficiency E% are given in **Table 7**. In the **Figure 11**, it can be seen that the Nyquist diagram shows an increase in the size of the semicircles with increasing concentration of GO inhibitor. This increase indicates an absorption of the GO inhibitor at the surface of the mild steel.

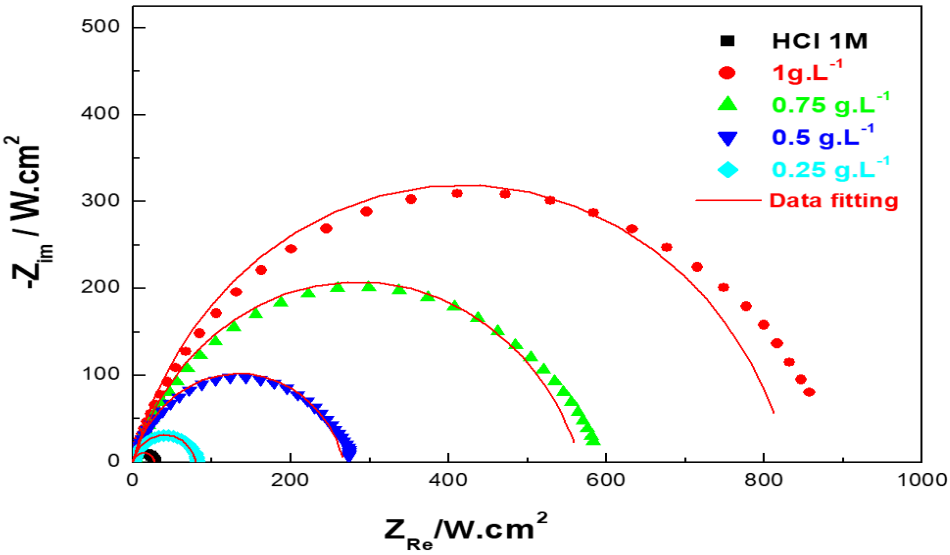

Figure 11. Nyquist curves of mild steel in 1 M HCl solution containing different concentrations of GO inhibitor at 25°C.

It appears from the results of **Table 7** that the increase in the concentration of the GO inhibitor is followed by the increase in the value of the efficiency to reach a maximum value of 96.68%.

Table 7. Electrochemical parameters from impedance curves for mild steel in a 1.0 M HCl solution with and without the addition of different concentrations of GO type II inhibitor at 25°C.

Medium	C (g/l)	Rs (Ω.cm2)	Rct (Ω.cm2)	Cdl (µF cm-2)	ndl	Q (µF.sn-1)	IEEIS (%)
HCl 1M	-	0.808	27.55	105.4	0.843	263.2	**---**
	1	1.126	831	52.55	0.835	88.01	**96.68**
GO/AD	0.75	0.970	566.4	56.14	0.806	109.6	**95.13**
	0.5	0.894	267	59.69	0.831	119.7	**89.68**
	0.25	0.670	80.15	73.85	0.846	162.3	**65.62**

3.2.2.2 Representation of impedance diagrams in the Bode plane

In order to acquire more information on the corrosion mechanisms and improve the previous results, bode plots of mild steel in 1.0 M HCl without and with different concentrations of GO at 25°C are shown in (**Figure 12**). It appears from the **Figure 12** that the phase angle plots become significantly broader in the high frequency range with increasing MA inhibitor concentration. In any case, it is clear that the Bode phase angle diagrams have only one maximum, i.e. a time constant corresponds to an adsorption corrosion process on the steel/solution interface.

3.2.2.3 Polarization method

The polarization curves of mild steel in a 1 M HCl solution without and with different concentrations of GO inhibitor are given in the **Figure 10**. It can be seen from the **Figure 13** that with increasing inhibitor concentration, there is a decrease in corrosion current (I_{corr}), which means that compound GO can affect both cathodic and anodic reactions.

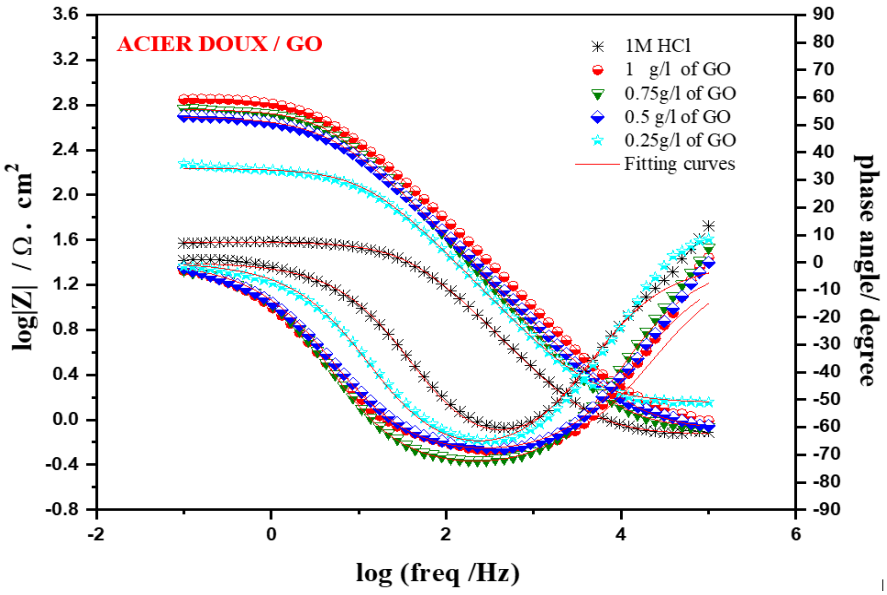

Figure 12. Bode representation of mild steel/1M HCl at different concentrations of GO inhibitor (25°C)

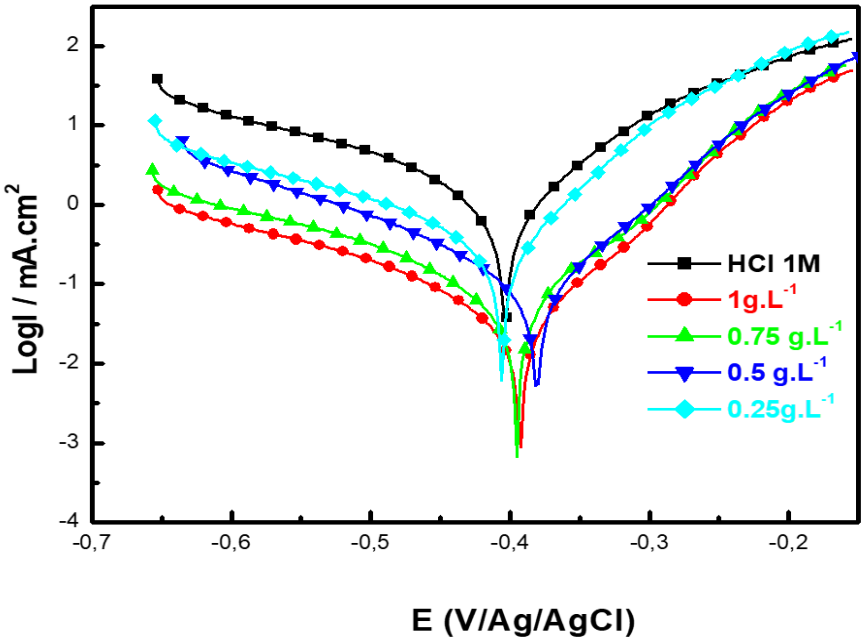

Figure 13. Polarization curves of mild steel in 1 M HCl solution containing different concentrations of GO inhibitor at 25°C.

Electrochemical parameters were determined and listed in **Table 8**. Based on the results reported in **Table 8**, the icorr decreased from 978 µA cm^{-2} to 36 µA cm^{-2} after addition of 1 M GO inhibitor. Also, it was noted that the %IEPDP increased with an increase in the concentrations of inhibitors to reach a maximum value of 96.31%, which is explained by a better adsorption of the molecules studied on the metal surface. Study of the inhibitory efficacy of polyphenol on HLE steel and Mild Steel in a corrosive medium of 1M HCl, is given on the **Table 9** and the **Table 10**. Based on the results obtained we could conclude that the efficiency of the two inhibitors is high, exceeding 92%. It is clear from **Table 9** and **Table 10** that the GO inhibitor is more effective than the MA inhibitor on mild steels and HLE steels.

Table 8. Electrochemical parameters derived from polarization curves for mild steel in 1.0 M HCl solution with and without the addition of different concentrations of GO inhibitor.

Medium	Concentration(M)	$-E_{corr}$ (mV/ECS)	I_{corr} (µA.cm−2)	$-\beta_c$ (mV.dec−1)	IE%
1M HCl	---	403	978	138	
GO /AD	1	392	36	141	**96.31**
	0.75	396	56	135	**94.27**
	0.5	380	102	138	**89.57**
	0.25	404	275	146	**71.88**

Table 9. Inhibitor Effectiveness on Mild Steel

	Inhibitory efficiency %	
	MA	**GO**
Gravimetry method	95%	95%
Impedance method	94.43%	96.68%
Polarization method	95.50%	96.31%

Table 10. Inhibitor Effectiveness on HLE Steel

	Inhibitory efficiency %	
	MA	**GO**
Gravimetry method	95%	95%
Impedance method	92.44%	94.86%
Polarization method	95.70%	95.23%

3.3 Surface analysis (SEM-EDX)

3.3.1 SEM for HLE steel with and without addition of MA and GO.

SEM analysis was used to observe the surface morphologies of HLE steel after 6 h of immersion in a 1.0 M HCl solution in the presence and absence of MA and GO. SEM images were obtained using the SEM quanta 200 scanning electron microscope. The scanning electron microscope (SEM) image of the polished HLE steel surface is shown in **Figure 11- (A, B, C)**.

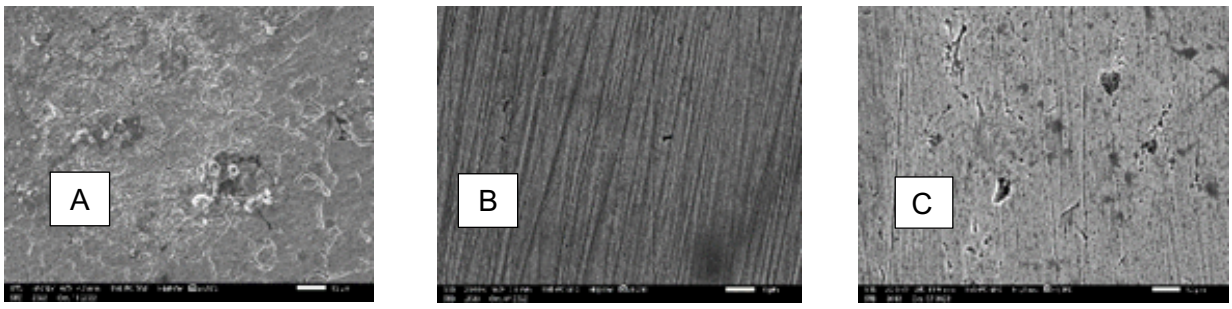

Figure 14 SEM morphology of the HLE steel surface: the steel after immersion in the 1 M HCl without inhibitor (A) the steel after immersion in the 1 M HCl acid solution in the presence of 10-3 M of MA (B). the steel after immersion in the 1 M HCl in the presence of 10^{-3} M GO (C).

The **Figure 14-A** reveals that the surface is badly corroded in the absence of the inhibitors due to the direct etching of the acid solution compared to the image obtained in the **Figure 14-B** which contains

the MA inhibitor and the **Figure 14-C** which contains GO inhibitor. This is due to the formation of a thin protective film of the inhibitor on the metal surface, which explains the effectiveness achieved by both MA and GO inhibitors.

3.3.2 SEM for mild steel with and without addition of MA and GO.

Surface analysis of the samples immersed in the uninhibited and inhibited solution for 6 h at 25°C was carried out to show the morphology and the nature of the atoms adsorbed on the surface of the mild steel. First, it can be observed from **Figure 15 A** that the sample after immersion in the acid medium showed remarkable damage to the steel surface compared to the surface morphology before the immersion time.

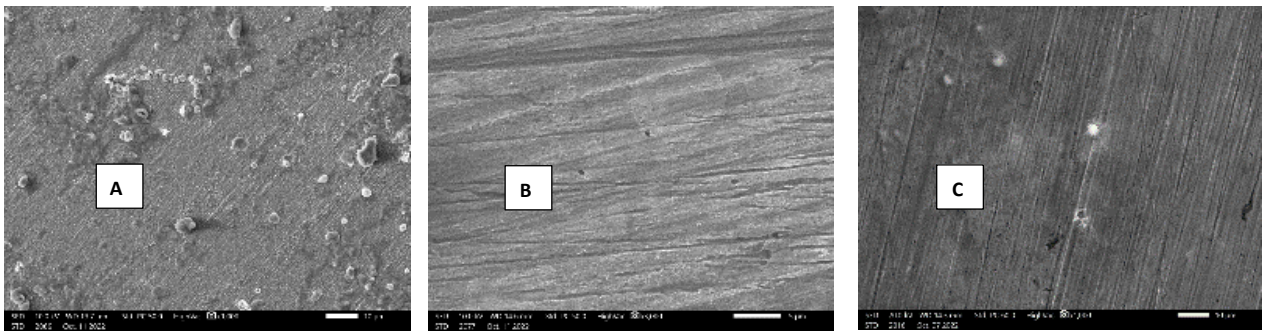

Figure 15 SEM morphology of the Mild steel surface: the steel after immersion in the 1M HCl solution without inhibitor (A) the steel after immersion in the 1 M HCl acid solution in the presence of 10-3 M of MA (B). the steel after immersion in the 1 M HCl solution in the presence of 10^{-3} M GO (C).

On the other hand, the samples obtained after their immersion in the inhibited solution were smoother compared to the morphology of the sample immersed in acidic media, which may be due to the formation of a heterogeneous protective layer formed by the adsorption of the studied MA and GO thus forming coordination bonds with the steel surface **Figures. 15 (A, B, C).**

3.3.3 EDX for HLE steel with and without addition of MA and GO.

The EDX technique based on the analysis of X-rays emitted during the electron-matter interaction was also carried out in order to understand the active sites responsible for the adsorption of the inhibitors studied. The EDX makes it possible to characterize the chemical element adsorbed on the surface of the steel after immersion in the corrosive medium with and without inhibitors.

3.3.3.1 EDX for HLE steel with and without addition of MA and GO inhibitors.

The EDX spectra of the steel after immersion in 1.0 M HCl without any inhibitors **(Figure 16**) show the major component of the existing elements on the surface. However, it can be noticed from the EDX recorded in the presence of GO that new peaks appear of manganese atoms (Mn) which act as active centers of these inhibitors for the adsorption and the formation of the film on the surface. steel. It is also assumed from The **Table 11** that the percentage of oxygen atomic content remarkably decreased for MA and GO and disappeared due to surface coverage by these compounds.

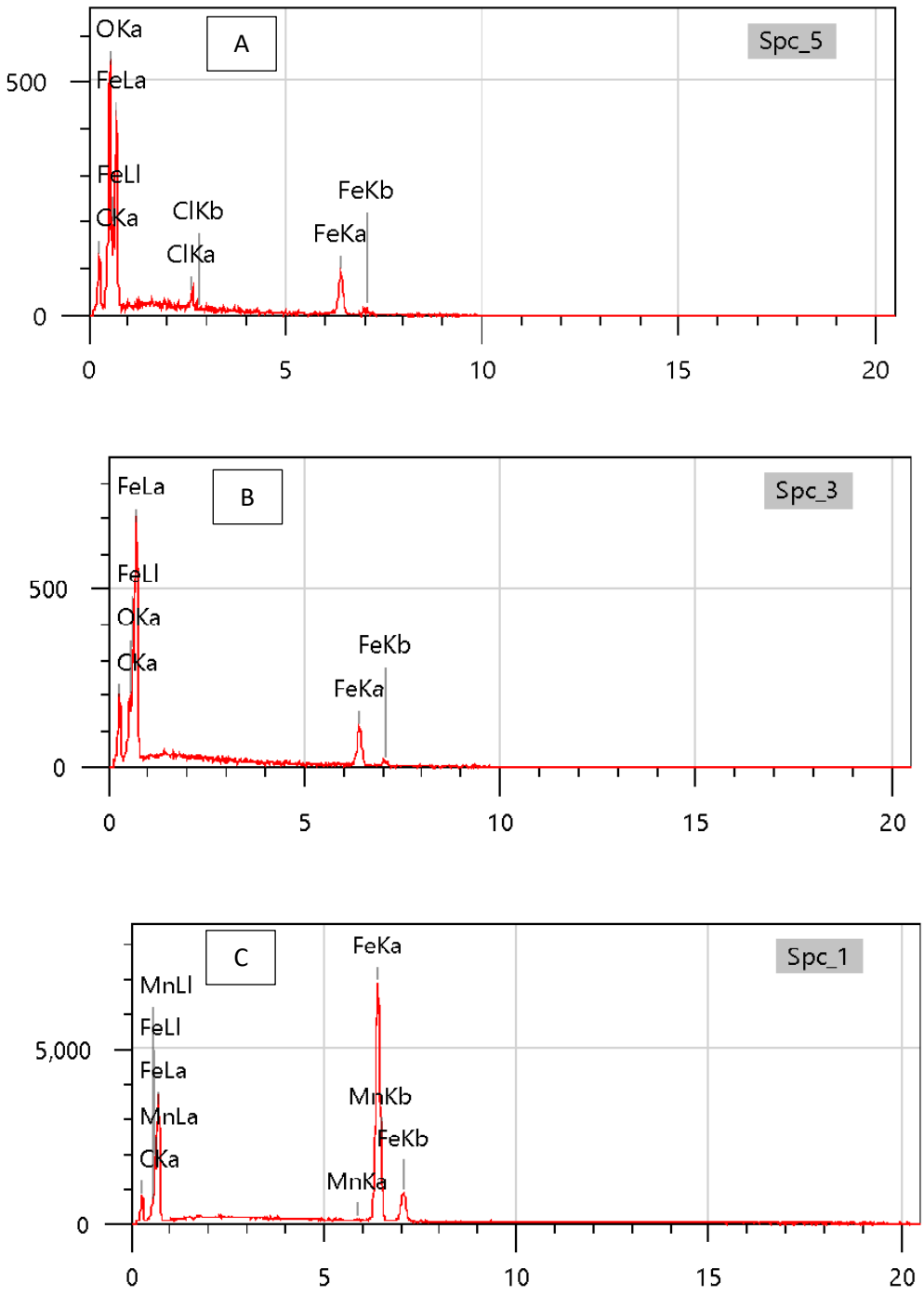

Figure 16. EDX spectra of HLE steel after immersion in 1.0 M HCl solution (A), after immersion in 1.0 M HCl solution containing 1.0 X 10-3 M of MA inhibitor (B), and after immersion in 1.0 M HCl solution containing 1.0 X 10-3 M of GO inhibitor (C).

Table 11. Percentage by weight of elements in HLE steel obtained from EDX analysis

	Fe	C	O	Cl	Mn	% Fe
AHLE without MA et GO	76.57	6.73	14.68	2.02		47.18
with MA	87.03	9.58	3.4			60.68
withGO	86.36	13.35			0.29	58.07

3.3.3.2 EDX for Midl steel with and without addition of MA and GO inhibitors.

It is observed from the **Figure 17** and the **Table 12** that various elements were detected by EDX analysis. In addition, a small percentage of manganese and carbon atoms was demonstrated in the presence of GO, which leads us to suggest that these atoms could be responsible for the interaction with the Mild Steel surface. Moreover, the percentage of iron atoms obtained from the solutions inhibited with MA is greater than that obtained from the aggressive solution (1.0 M HCl).

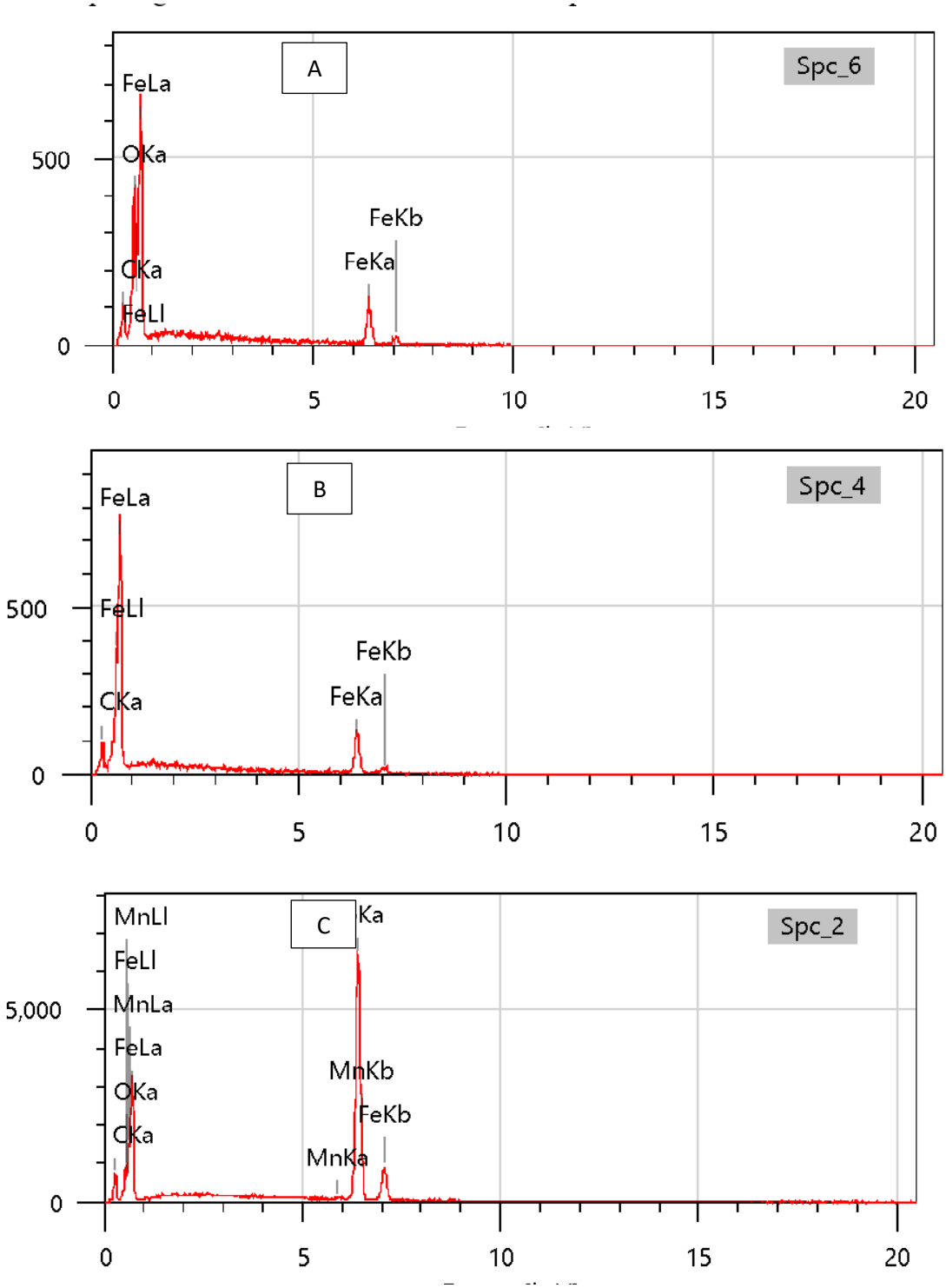

Figure 17. EDX spectra of Mild steel after immersion in 1.0 M HCl solution (A), after immersion in 1.0 M HCl solution containing 1.0 X 10^{-3} M of MA inhibitor (B), and after immersion in 1.0 M HCl solution containing 1.0 X 10^{-3} M GO inhibitor (C).

Thus, it can be concluded from the EDX microanalysis that the MA and GO studied are adsorbed on the surface of the samples by the manganese atom and the C = C bonds forming a layer of protective film and confirming the good behavior of these molecules. when in contact with the aggressive solution.

Table 12 Percentage by weight of elements in HLE steel obtained from EDX analysis

	Fe	C	O	Cl	Mn	Fe %
AD without MA and GO	87.69	4.01	8.3			64.81
with MA	96.15	3.85				84.31
with GO	83.37	12.18	3.97		0.48	54.01

Conclusion

The experiments revealed that the polyphenol extracted from vegetable water MA and extracted from pomace GO behaved as mixed type inhibitors. This study was performed using the weight loss method, potentiodynamic polarization and electrochemical impedance spectroscopy (EIS). The polyphenol extracted from vegetable waters inhibits the corrosion of HLE steel and mild steel in 1M HCl. The efficiency of inhibition increases with increasing inhibitor concentrations to reach a maximum value of 95.7% for HLE steel and a maximum value of 95.50% for mild steel. For the polyphenol extracted from olive pomace, it inhibits the corrosion of HLE steel and mild steel in 1M HCl. The efficiency increases with increasing inhibitor concentrations to reach a maximum value of 96.68% for mild steel and a maximum value of 95.23% for HLE steel. According to the Langmuir isothermal model and the thermodynamic parameters, the inhibitors MA and GO were adsorbed on the surfaces of HLE and mild steels by physical and chemical bonds. SEM and EDX examinations proved the formation of a protective layer of adsorbed inhibitors on the steel surface. At the end of the results obtained during this work we propose a contribution of solution to two major problems which are on the one hand the management of the waste sources of pollution of the various mediums and their valorization in alternative materials of the organic inhibitors synthesized for inhibition of corrosion. And on the other hand, to fight against the corrosion of steels by the use of green inhibitors in order to increase the life of the steels used in the Moroccan automotive industry.

Acknowledgement: The technical inputs of Mr Aziz CHAMI are acknowledged.

Disclosure statement: *Conflict of Interest:* The authors declare that there are no conflicts of interest.

Compliance with Ethical Standards: This article does not contain any studies involving human or animal subjects.

References

Abdulbasit Y.U., Abdullahi B. U. and Bishir U. (2023). Experimental and Theoretical Evaluation of Corrosion Inhibition Performance of Senna Obtusifolia Leaves Extract on Mild Steel In 0.5M HCl, *Mor. J. Chem.*, 14(2), 282-299. doi: https://doi.org/10.48317/IMIST. PRSM/morjchem-v11i2.38203

About H., El Faydy M., Benhiba F., Kerroum Y., Kaichouh G., Oudda H., Guenbour A., LakhrissiB., Warad I., Zarrouk A. (2021). Experimental and empirical assessment of two new 8-hydroxyquinoline analogs as effective corrosion inhibitor for C22E steel in 1 M HCl, *J. Mol. Liq.*, 325, 114644. doi: https://doi.org/10.1016/j.molliq.2020.114644

Abubakar M.S. and Usman B. (2019). Investigation of Corrosion Inhibition Potential of Ethanol Extract Balanites aegyptiaca Leaves on Mild Steel in 1M Hydrochloric Acid, *Mor. J. Chem.*, 7(1), 82-97. doi: https://doi.org/10.48317/IMIST.PRSM/morjchem-v7i1.14889

Al-Mazaideh G.M., Al-Quran S.A. (2018). Inhibitive action of Chamomile extract on the corrosion of Iron: Density functional theory, *Moroccan Journal of Chemistry* 6(1), 195-202

Akande I. G., Fayomi O. S. I., Okore P. N. (2023). Investigation of the microstructure, corrosion resistance and hardness of bone particle reinforced cast iron for engine blocks application in automotive and marine industries, *Hybrid Advances*, 2, 100022, https://doi.org/10.1016/j.hybadv.2023.100022

Belghiti M.E., Karzazi Y., Dafali A., Obot I.B., Ebenso E.E., Emrane K.M., Bahadur I., Hammouti B., Bentiss F. (2016). Anti-corrosive properties of 4-amino-3,5-bis(disubstituted)-1,2,4-triazole derivatives on mild steel corrosion in 2 M H_3PO_4 solution: Experimental and theoretical studies, *J. Mol. Liq*., 2016, 874–886. doi: https://doi.org/10.1016/j.molliq.2015.12.093

Bouayad K., Kandi Rodi Y., El Ghadraouni E. H., Elmsellem H., Ouzidan Y., El Mahi B., Essassi E. M., Abdel-Rahman I., Chetouani A., Hammouti B. (2017). Corrosion Protection of Mild Steel in Hydrochloric Acid at 308 K using Benzimidazole Derivatives: Weight Loss, Adsorption and Quantum Chemical Studies, *Mor. J. Chem*., 5(2), 285-296, doi: https://doi.org/10.48317/IMIST.PRSM/morjchem-v5i2.8326

Bourichi S., KandriRodi Y., Elmsellem H., Steli H., Ouzidan Y., Sebbar N.K., OuazzaniChahdi F., Essassi E.M., El-Hajjaji F., Hammouti B. (2016). 3-Allyl-6-bromo-2-(4-methoxyphenyl)-3H-imidazo[4,5-b]pyridine as a potential inhibitor for Corrosion of mild steel in in 1.0 HCl solution, *Der. Pharma. Chem*., 8(10), 179–186, doi: http://derpharmachemica.com/archive.html

Chai C., Xu Y., Li D., Zhao X., Xu Y., Zhang L. (2019). Cysteamine modified polyaspartic acid as a new class of green corrosion inhibitor for mild steel in sulfuric acid medium: synthesis, electrochemical, surface study and theoretical calculation, *Prog. Org. Coat.,* 129 159–170, https://doi.org/10.1016/j.porgcoat.2018.12.028

Chami A., Benabbou R., Taleb M., Rais Z., El Haji M. (2020). ELECTRE multi-criteria analysis for choosing material concerned by the corrosion problem in automotive industry, *J. Appl. Sci. Envir. Stud*. 3(3), 132-146, doi: https://revues.imist.ma/index.php/JASES/article/view/20393

Chami A., Benabbou R., Taleb M., Rais Z., El Haji M. (2021). Analysis of survey data on corrosion in the automotive industry, *Materials Today: Proceedings*, doi: https://doi.org/10.1016/j.matpr.2021.03.113.

Chami A., Benabbou R., Taleb M., Rais Z., El Haji M. (2021). Experimental approach of polyphenol as an ecological corrosion inhibitor in HCl 1M for steel used in the Moroccan automotive industry, *Journal of Corrosion Science and Engineering*, 2021, 23 P87, doi: https://www.jcse.org/viewPaper/ID/1700/rygL6BXB36IEVTWQEozr5bf94HmOGR

Chami A., Benabbou R., Taleb M., Rais Z., El Haji M. (2021). Review of the green inhibitors for steel corrosion in automotive industry, *Journal of Corrosion Science and Engineering*, 23, 68, doi: https://www.jcse.org/viewPaper/ID/1677/yQbUrdh1J3B4gsaEzk1V8RfpVPYoSf

Chaubey N., Qurashi A., Chauhan D.S., Quraishi M.A. (2021). Frontiers and advances in green and sustainable inhibitors for corrosion applications: A critical review, *Journal of Molecular Liquids* 321, 114385

Chetouani A., Aouniti A., Hammouti B., Benchat N., Benhadda T. and Kertit S. (2003). Corrosion Inhibitors for Iron in Hydrochloride Acid Solution by Newly Synthesised Pyridazine Derivatives, *Corrosion Science*, 45(8), 1675-1684. doi: https://doi.org/10.1016/S0010-938X(03)00018-0

Dermeche S., Nadour M., Larroche C., Moulti-Mati F., and Michaud P., (2013). Olive mill wastes: biochemical characterizations and valorization strategies, *Process Biochemistry*, 48(10), 1532–1552, doi: https://doi.org/10.1016/j.procbio.2013.07.010

El aoufir Y., El Bakri Y., Kerroum, Lgaz H., Harmaoui A., Chefouani A., Sebhaoui J., Salghi R., Ramli Y., Guenbour A., Essassi E. M., Oudda H. (2017). Triazole derivative as new and effective corrosion inhibitor for carbon steel in hydrochloric acid: Electrochemical and quantum chemical studies, *Mor. J. Chem*., 5(4), 545 – 559, doi: https://doi.org/10.48317/IMIST.PRSM/morjchem-v5i4.8979

EL Aoufir Y., Lgaz H., Bourazmi H., Kerroum Y., Ramli Y., Guenbour A., Salghi R., El-Hajjaji F., Hammouti B., Oudda H. (2016). Quinoxaline Derivatives as Corrosion Inhibitors of Carbon Steel in Hydrochloridric Acid Media: Electrochemical, DFT and Monte Carlo simulations studies, *J. Mater. Environ. Sci.* 7, 4330–4347, doi: http://www.jmaterenvironsci.com

El Faydy M., About H., Warad I., Kerroum Y., Berisha A., Podvorica F., Bentiss F., Kaichouh G., Lakhrissi B., Zarrouk A. (2021). Insight into the corrosion inhibition of new bis-quinolin-8-ols derivatives as highly efficient inhibitors for C35E steel in 0.5 M H_2SO_4, *J. Mol. Liq*. 342, 117333, doi: https://doi.org/10.1016/j. molliq.2021.117333

El Faydy M., Benhiba F., Lakhrissi B., Touhami M.E., Warad I., Bentiss F., Zarrouk A. (2019). The inhibitive impact of both kinds of 5-isothiocyanatomethyl-8- hydroxyquinoline derivatives on the corrosion of carbon steel in acidic electrolyte, *J. Mol. Liq.* 295, 111629, doi:

https://doi.org/10.1016/j.molliq.2019.111629
El Ouali I., Chetouani A., Hammouti B., Aouniti A., Touzani R., El Kadiri S. (2013). Thermodynamic Study and Characterization by Electrochemical Technique of Pyrazole Derivatives as Corrosion Inhibitors for C38 Steel in Molar Hydrochloric Acid, *Portugaliae Electrochimica Acta.* 31(2), 53-78, doi: https://doi.org/10.4152/pea.201302053
Elmsellem H., Aouniti A., Khoutoul M., Chetouani A., Hammouti B., Benchat N., Touzani R., Elazzouzi M. (2014). Theoretical approach to the corrosion inhibition efficiency of some pyrimidine derivatives using DFT method of mild steel in HCl solution, *J. Chem. Pharm. Res.,* 6(4), 1216-1224
Ezeh E.M., Chinedu Agu P., (2023). Assessment of the Corrosion inhibitory potentials of Chromolaena odorat leaf extract on mild steel in hydrogen chloride acid environment, *Mor. J. Chem.,* 14(1), 188-204. https://doi.org/10.48317/IMIST.PRSM/morjchem-v10i3.30521
Ghazoui A., Benchat N., El-Hajjaji F., Taleb M., Rais Z., Saddik R., Elaatiaoui A., Hammouti B. (2016). The study of the effect of ethyl (6-methyl-3-oxopyridazin-2-yl) acetate on mild steel corrosion in 1M HCl, *J. Alloys Compounds* 693, 510–517, doi: https://doi.org/10.1016/j.jallcom.2016.09.191
Guo L., Zhu S., Zhang S., He Q., Li W. (2014). Theoretical studies of three triazole derivatives as corosion inhibitors for mild steel in acidic medium, *Corros. Sci.* 87, 366–375, doi: https://doi.org/10.1016/j.corsci.2014.06.040
Laabaissi T., Benhiba F., Rouifi Z., Missioui M., Ourrak K., Oudda H., Ramli Y., Warad I., Allali M., Zarrouk A. (2019). New quinoxaline derivative as a green corrosion inhibitor for mild steel in mild acidic medium: electrochemical and theoretical studies, *Int. J. Corros. Scale Inhib.* 8, 241–256, doi: https://doi.org/10.17675/ 2305-6894-2019-8-2-6.
Leach F., Kalghatgi G., Stone R., Miles P. (2020). The scope for improving the efficiency and environmental impact of internal combustion engines, *Transportation Engineering,* 100005, ISSN 2666-691X, https://doi.org/10.1016/j.treng.2020.100005
Li S., Zhao Y., Wan H., Lin J., Min J. (2023). Molecular Understanding of the Interfacial Interaction and Corrosion Resistance between Epoxy Adhesive and Metallic Oxides on Galvanized Steel. *Materials,* 16, 3061. https://doi.org/10.3390/ma16083061
Ma Y., Yang M., Yuan F., Wu X. (2019). A review on heterogeneous nanostructures: a strategy for superior mechanical properties in metals, *Metals.* 9, 1–32, doi: https://doi.org/10.3390/met9050598
Mbamalu E.E., Chinedu A.P. (2023). Assessment of the Corrosion Inhibitory Potentials of Chromolaena Odorata Leaf Extract on Mild Steel in Hydrogen Chloride Acid Environment, Moroccan Journal of Chemistry 11(1), pp. 188-204
Musa A.Y., Jalgham R.T.T., Mohamad A.B. (2012). Molecular dynamic and quantum chemical calculations for phthalazine derivatives as corrosion inhibitors of mild steel in 1M HCl, *Corros. Sci*. 56 176–183, doi: https://doi.org/10.1016/j.corsci.2011.12.005
Ouakki M., Galai M., Rbaa M., Abousalem A.S., Lakhrissi B., Rifi E.H., Cherkaoui M. (2019). Quantum chemical and experimental evaluation of the inhibitory action of two imidazole derivatives on mild steel corrosion in sulphuric acid medium, *Heliyon* 5(11), e02759, doi: https://doi.org/10.1016/j.heliyon.2019.e02759
Popoola L.T. (2019). Organic green corrosion inhibitors (OGCIs): a critical review, *Corrosion Rev*. 37, 71–102, doi: https://doi.org/10.1515/corrrev-2018-0058
Rbaa M., Benhiba F., Obot I.B., Oudda H., Warad I., Lakhrissi B., Zarrouk A. (2019). Two new 8-hydroxyquinoline derivatives as efficient corrosion inhibitors for mild steel in hydrochloric acid: synthesis, electrochemical, surface morphological, UV–visible and theoretical studies, *J. Mol. Liq.* 276, 120–133, doi: https://doi. org/10.1016/j.molliq.2018.11.104.
Salhi A., Bouyanzer A., El Mounsi I., Bendaha H., Chetouani A., Amhandi H., Zarrouk A., Hammouti B., Desjobert J. M.,Costa J. (2016). The inhibitive action of Pistacia lentiscus as a potential green corrosion inhibitor for mild steel in acidic medium, *Mor. J. Chem*., 4(4) 1037 – 1051, doi: https://doi.org/10.48317/IMIST.PRSM/morjchem-v4i4.6898
Saraswat V., Kumari R., Yadav M. (2022). Novel carbon dots as efficient green corrosion inhibitor for mild steel in HCl solution: electrochemical, gravimetric and XPS studies, *J. Phys. Chem. Solid.* 160, 110341, doi: https://doi.org/10.1016/j. jpcs.2021.110341
Tan B., Zhang S., Cao X., Fu A., Guo L., Marzouki R., Li W. (2022). Insight into the anticorrosion performance of two food flavors as eco-friendly and ultra-high-performance inhibitors for copper in sulfuric acid medium, *J. Colloid Interface Sci*. 609, 838–851, doi: https://doi.org/10.1016/j.jcis.2021.11.085.
Torres Hernández J.R., Del Angel Meraz E. and Corvo Perez E.F. (2023). Tradescantia spathacea: New green

corrosion inhibitor for SAE 1010 steel in acid medium, *Int. J. Corros. Scale Inhib.,* 12(1), 61-83 doi: 10.17675/2305-6894-2023-12-1-4

Ugi B. U., Obeten M. E., Bassey V. M., BoEkom E.J., Omaliko E. C., Ugi F. B., Uwah I.E. (2021). Quantum and Electrochemical Studies of Corrosion Inhibition Impact on Industrial Structural Steel (E410) by Expired Amiloride Drug in 0.5 M Solutions of HCl, H_2SO_4 and $NaHCO_3$, *Mor. J. Chem*. 9(4), 677-696, doi: https://doi.org/10.48317/IMIST.PRSM/morjchem-v9i3.22346

Verma C., Ebenso E.E., Quraishi M.A. (2017). Ionic liquids as green and sustainable corrosion inhibitors for metals and alloys: an overview, *J. Mol. Liq.* 233, 403–414, doi: https://doi.org/10.1016/j.molliq.2017.02.111

Zerfaoui M., Hammouti B., Oudda H., Benkaddour M. (2014). Inhibition of corrosion of iron in citric acid media by aminoacids, *Prop. Org. Coat.* 51N°2, 134-138

(2023) ; https://revues.imist.ma/index.php/morjchem/index